dissociation of all the three precursors. However, daughter spectra taken after interaction of this mass-selected ion with the surface show peaks at mass-to-charge ratios of approximately twice its value, and these peaks can only be due to singly charged ions produced from the incident doubly charged $[C_6H_6]^{2+}$ ion. The fragment ions of mass-to-charge ratio 39 and below in the SID daughter spectra may originate from both the doubly charged $[C_6H_6]^{2+}$ ion and the 39+ ion, and hence only the ions above m/z 39 in the SID daughter spectra are considered in the discussion that follows.

Three points are noteworthy: (i) The charge-exchange process gives much more abundant product ions for benzene than for the acyclic isomers; products of charge exchange appear in the relative ratio of 15:2.5:1 for benzene, 2,4-hexadiyne, and 1,5-hexadiyne, respectively. (ii) The daughter spectra are different, although they show the presence of the same fragment ions. (iii) The benzene spectrum is quite similar to the SID daughter spectrum of the benzene molecular ion recorded at 60-eV collision energy. The difference in charge-exchange efficiency suggests that the $[C_6H_6]^{2+}$ ion derived from benzene is quite different from that of the acyclic isomers. This difference might be attributed to the presence of the cyclic structure, which has been proposed as the stable ion structure.[32,33] The similarity to the daughter spectrum of the singly charged benzene molecular ion, which is presumed to have a mixture of structures most of which are cyclic, further supports this interpretation.

Conclusion

It is evident that surface-induced reactions are a useful tool in the distinction of isomeric ions, including the $[C_6H_6]^{\bullet+}$ ions derived from benzene, 2,4-hexadiyne, and 1,5-hexadiyne. The salient findings of this study are as follows: (i) The three $[C_6H_6]^{\bullet+}$ isomeric ions are structurally distinct as is evident, for example, in difference spectra plotted for collision energies that range from 25 to 150 eV. While these results indicate that the three compounds yield distinct isomeric structures, partial isomerization is not excluded. The ions studied in this experiment, like those examined by charge stripping,[24] are stable to fragmentation. Furthermore, because of the large energy deposition,[16,40] they are likely to be drawn from deep in the potential energy well and to be stable also to isomerization. This is probably not the case for the stable ions examined by other methods which consequently do display isomerization, especially cyclization of ionized 1,5-hexadiyne.[25,29,30] (ii) Fragmentation efficiencies of the isomeric ions provide additional information that facilitates distinction between the isomers. (iii) The expected[16,40] high internal energy deposition in SID is evident. At 150 eV, large abundances of methyl cation in the daughter spectra of 2,4-hexadiyne molecular ion and small abundances in the case of benzene and 1,5-hexadiyne molecular ions are observed. It is significant that the only ion among the isomers which has terminal methyl groups is that derived from 2,4-hexadiyne. (iv) However, with the exception of $[CH_3]^+$ (m/z 15), the 150-eV spectra are nearly identical for all three isomers, thus demonstrating that maximization of energy deposition is not always desirable in structural differentiation. (v) Ion/surface reactions provide important additional information in distinguishing isomeric ions. On the basis of the abundances of the peak of m/z 91, presumably due to $CH_3^{\bullet}$ abstraction from the adsorbate by the incident $[C_6H_6]^{\bullet+}$ ions, followed by loss of H_2, benzene-derived $[C_6H_6]^{\bullet+}$ ions can be distinguished easily from the other isomers. (vi) Finally, charge exchange of $[C_6H_6]^{2+}$ from benzene at the surface yields a singly charged ion which has the (presumably cyclic) structure of singly ionized benzene.

Acknowledgment. We acknowledge the support of the National Science Foundation (Grant CHE 85-21634).

Registry No. Benzene, 71-43-2; benzene radical cation, 34504-50-2; benzene dication, 15157-23-0; 1,5-hexadiyne, 628-16-0; 1,5-hexadiyne radical cation, 61369-11-7; 2,4-hexadiyne, 2809-69-0; 2,4-hexadiyne radical cation, 61369-13-9.

Time-Resolved EPR Studies of the Properties of the Triplet-State Enols of Intramolecularly Hydrogen-Bonded *o*-Hydroxybenzaldehyde and Related Molecules

Seigo Yamauchi* and Noboru Hirota*

Contribution from the Department of Chemistry, Faculty of Science, Kyoto University, Kyoto 606, Japan. *Received July 22, 1987*

Abstract: Time-resolved EPR (TREPR) studies were made on the lowest excited triplet (T_1) states of the intramolecularly hydrogen-bonded molecules *o*-hydroxybenzaldehyde (OHBA), *o*-hydroxyacetophenone (OHAP), 7-hydroxy-1-indanone (7HIN), and salicylamide (SAM) in polar and nonpolar solvents and in single crystals of durene at 77 K. In almost all systems TREPR spectra were obtained. Emission and excitation spectra were also observed in the same systems to assist in the identification of the species involved. Very similar TREPR spectra were obtained for all the molecules studied and were assigned as those of $^3\pi\pi^*$ enols on the basis of the determined zero-field (zf) triplet sublevel schemes, polarization properties, and the emission and excitation characteristics. The triplet sublevel schemes and the $S_1 \rightarrow T_1$ intersystem crossing (isc) ratios were obtained by magnetophotoselection experiments in a methylcyclohexane glass and by the angular dependence of the TREPR signals in a single crystal of durene. Small zero-field splittings (zfs) and unusual isc ratios were obtained for these systems, which was interpreted by considering locations of the higher $^3n\pi^*$ and $^3\sigma\pi^*$ states. A mechanism of the enolization process is discussed by comparing the TREPR spectra of the neutral and anion forms of 7HIN. Different types of TREPR spectra were obtained for OHBA and 7HIN in a mixed solvent of ethanol and toluene (1:1) and were assigned as those of $^3\pi\pi^*$ keto forms.

Excited-state dynamics of intramolecularly hydrogen-bonded molecules is a topic of current interest, and various spectroscopic techniques have been employed to study this problem. The techniques used include picosecond spectroscopy,[1] two-step laser excitation (TSLE) spectroscopy,[2] transient absorption spectroscopy of a nanosecond time scale,[3] and high-resolution fluorescence spectroscopy.[4] Interesting details about dynamics and structures

(1) (a) Hou, S. Y.; Hetherington, W. M., III; Korenowski, G. M.; Eisenthal, K. B. *Chem. Phys. Lett.* **1979**, *68*, 282. (b) Smith, K. K.; Kaufmann, K. J.; *J. Phys. Chem.* **1978**, *82*, 2286. (c) Barbara, P. F.; Rentzepis, T. M.; Brus, L. E. *J. Am. Chem. Soc.* **1980**, *102*, 2786. (d) Kosower, E. M.; Huppert, D. *Annu. Rev. Phys. Chem.* **1986**, *37*, 127.

(2) (a) Itoh, M.; Fujiwara, Y. *J. Phys. Chem.* **1983**, *87*, 4558. (b) Itoh, M.; Yoshida, Y.; Takahashi, M. *J. Am. Chem. Soc.* **1985**, *107*, 4819. (c) Tokumura, K.; Watanabe, Y.; Itoh, M. *J. Phys. Chem.* **1986**, *90*, 2362.

(3) (a) Haag, R.; Wirz, J.; Wagner, P. J. *Helv. Chim. Acta* **1977**, *60*, 2595. (b) Scaiano, J. C. *Acc. Chem. Res.* **1982**, *15*, 252. (c) Mordzinski, A.; Grellmann, K. H. *J. Phys. Chem.* **1986**, *90*, 5503.

0002-7863/88/1510-1346$01.50/0

of the excited singlet states of such molecules have been obtained recently. In our laboratory we have investigated *o*-hydroxybenzaldehyde (OHBA), *o*-hydroxyacetophenone (OHAP), salicylamide (SAM), methyl salicylate (MS), and 7-hydroxy-1-indanone (7HIN).[5-8] These molecules are intramolecularly hydrogen-bonded in the keto forms in the ground states, but upon UV excitation they undergo isomerization via excited-state proton transfer and emit Stokes-shifted fluorescence. Previous investigations have provided information about the rates of proton transfer as well as of nonradiative decay processes[5,6] and qualitative features of the potential surfaces of the ground and excited states.[7,8] However, there remain uncertain aspects about structures of the proton-transferred species, though the results of our fluorescence studies are consistent with the enol structures.[8] In these studies attention was mainly focused on the excited singlet states.

Involvement of the excited triplet states in the excitation–decay cycles of the intramolecularly hydrogen-bonded molecules has been mentioned in several works.[3,7] For example, triplet states of the enol tautomers were invoked to explain the observed transient absorption spectra of OHAP, SAM, and 7HIN.[7] However, little is known about such triplet states, mainly because these species are nonphosphorescent. To our knowledge no EPR study has been reported on the enol type tautomers.

Over the past several years we have applied time-resolved EPR (TREPR) with laser excitation to elucidate the properties of nonphosphorescent short-lived triplet states.[9] This technique has proved to be extremely useful for this purpose. Therefore, nonphosphorescent short-lived triplet states of intramolecularly hydrogen-bonded molecules appear to be an attractive object for the TREPR study. It is hoped that the TREPR study clarifies the nature of the triplet states existing under various conditions and provides useful information about electronic and molecular structures of the enol type triplet states. This paper describes our attempts toward such a goal.

In the present study we have succeeded in obtaining transient EPR spectra of OHBA, OHAP, 7HIN, and SAM in polar (ethanol + toluene (EtOH + Tol)) and nonpolar (methylcyclohexane (MCH)) solvents as well as in mixed crystals of durene at 77 K and examined their properties in detail. We have also examined the emission and excitation spectra of the fluorescence and phosphorescence in the same systems to correlate the EPR spectra with the emission properties. On the basis of these experimental results we have identified the EPR spectra of the enol tautomers, which are characterized by small zero-field splittings (zfs) and unique polarization patterns. Here we discuss the triplet sublevel schemes, the directions of the principal axes of the zf tensors, and the polarization of the triplet signals in connection with the structures and pathway to form the enol triplet states.

Experimental Section

The methods of purification and preparation of solute molecules have already been described in previous papers.[5,6] Solvents (MCH, EtOH, and Tol) were spectrograde and were used without further purification. As a polar solvent we used a 1:1 mixture of EtOH and Tol. Single cyrstals of durene were grown by the Bridgman method and cut along the molecular axes of durene by observing isogeric patterns with a Nikon 104 polarizing microscope.

TREPR signals were obtained in the following way.[9] A sample in a microwave cavity was irradiated with a Lumonics TE-861M excimer laser (XeCl, 308 nm, ~40 mJ/pulse). The photoinduced transient EPR signals amplified by a preamplifier of a microwave unit (JEOL FE-3X) were fed to a PAR 160 boxcar integrator, and the TREPR spectra were observed mostly at 0.4 μs after the laser pulse. The time resolution of our system was ca. 0.1 μs. Magnetophotoselection experiments were performed by using polarized light obtained by passing the laser light through a Glan–Thompson prism. All measurements were made at 77 K using a finger tip Dewar.

Emission and excitation spectra for the fluorescence and phosphorescence were obtained with a Shimadzu PF502 spectrometer. Phosphorescence lifetimes were measured by exciting the samples with the laser, detecting the signals with an EMI 9502B photomultiplier through a Spex 1704 1-m monochromator, and analyzing the decay curves with a Kawasaki Electronica MR50E transient memory and a TM700 signal averager.

Table I. Various Kinds of Emissions Observed at 77 K[a]

OHBA	OHAP	7HIN	SAM
	MCH		
enol Fl $^3n\pi^*$ Ph	enol Fl	enol Fl $^3n\pi^*$ Ph	enol Fl
	EtOH + Tol		
$^3\pi\pi^*$ Ph	enol Fl $^3\pi\pi^*$ Ph	$^3\pi\pi^*$ Ph anion Fl	enol Fl $^3\pi\pi^*$ Ph

[a] Fl and Ph denote fluorescence and phosphorescence, respectively. The intensity of the lower emission is weaker than that of the higher emission.

Results

1. Emission and Excitation Spectra. We have examined the emission and excitation spectra of 7HIN and SAM in polar (EtOH + Tol) and nonpolar (MCH) solvents at 77 K. The results for the emissions are summarized in Table I together with those already reported for OHBA and OHAP.[5,6] Various kinds of emissions were observed in these systems. The Stokes-shifted fluorescence observed in nonpolar solvents was ascribed to the enol tautomer,[5] and we call this type of fluorescence an enol type. In polar solvents an additional fluorescence was observed with an emission maximum at a shorter wavelength than that of the enol type one. This fluorescence was assigned as an anion fluorescence.[7] Two kinds of phosphorescence of an aromatic carbonyl were observed and were classified into two types, $^3\pi\pi^*$ and $^3n\pi^*$ type phosphorescence, respectively, on the basis of the spectral features.[10] The main observations about the emissions and their excitation spectra are summarized as follows.

(1) In MCH the enol type fluorescence was observed in all the molecules studied. Additionally, the $^3n\pi^*$ type phosphorescence was observed in OHBA and 7HIN.

(2) The $^3\pi\pi^*$ type phosphorescence was observed for all the molecules in EtOH + Tol, in which the enol type fluorescence was observed only for OHAP and SAM.

(3) When NaOH (~10^{-2} M) was added to the 7HIN/(EtOH + tol) system, the intensity of the anion fluorescence (λ_{max} ~ 437 nm) increased and the anion phosphorescence (λ_{max} ~ 470 nm) appeared, the $^3\pi\pi^*$ phosphorescence still being observed. The shapes of the anion fluorescence and phosphorescence spectra were very similar with identical excitation spectra.

(4) The excitation spectra were different for three kinds of emissions, namely, the enol type fluorescence, the $^3\pi\pi^*$ and $^3n\pi^*$ type phosphorescence, and the anion type fluorescence as shown in Figure 1. The excitation peaks of the enol fluorescence are located at slightly longer wavelengths than those of the phosphorescence and at much shorter wavelengths than those of the anion fluorescence.

(5) As reported previously,[8] only the enol type fluorescence was observed in mixed crystals of durene.

2. TREPR Measurements. We observed TREPR spectra of OHBA, OHAP, 7HIN, and SAM in MCH and EtOH + Tol at 77 K. Some typical spectra in MCH observed at 0.4 μs after laser excitation are shown in Figure 2. In all the systems resonance fields for H_{min} transitions and two pairs of $\Delta m = \pm 1$ transitions

(4) (a) Goodman, J.; Brus, L. E. *J. Am. Chem. Soc.* **1978**, *100*, 7472. (b) Felker, P. M.; Lambert, W. R.; Zewail, A. H. *J. Chem. Phys.* **1982**, *77*, 1603. (c) Heimbrook, L.; Kenny, J. E.; Kohler, B. E.; Scott, G. W. *J. Phys. Chem.* **1983**, *87*, 280.

(5) Nagaoka, S.; Hirota, N.; Sumitani, M.; Yoshihara, K. *J. Am. Chem. Soc.* **1983**, *105*, 4220.

(6) Nagaoka, S.; Hirota, N.; Sumitani, M.; Yoshihara, K.; Lipczysnska-Kochany, E.; Iwamura, H. *J. Am. Chem. Soc.* **1984**, *106*, 6913.

(7) Nishiya, T.; Yamauchi, S.; Hirota, N.; Fujiwara, Y.; Itoh, M. *J. Am. Chem. Soc.* **1986**, *108*, 3880.

(8) Nishiya, T.; Yamauchi, S.; Hirota, N.; Baba, M.; Hanazaki, I. *J. Phys. Chem.* **1986**, *90*, 5730.

(9) Terazima, M.; Yamauchi, S.; Hirota, N. *J. Phys. Chem.* **1985**, *89*, 1220; *J. Chem. Phys.* **1985**, *83*, 3234; **1986**, *84*, 3679.

(10) (a) Harrigan, E. T.; Hirota, N. *Mol. Phys.* **1976**, *31*, 681. (b) Goodman, L.; Lamotle, M.; Koyanagi, M. *Chem. Phys.* **1980**, *47*, 329.

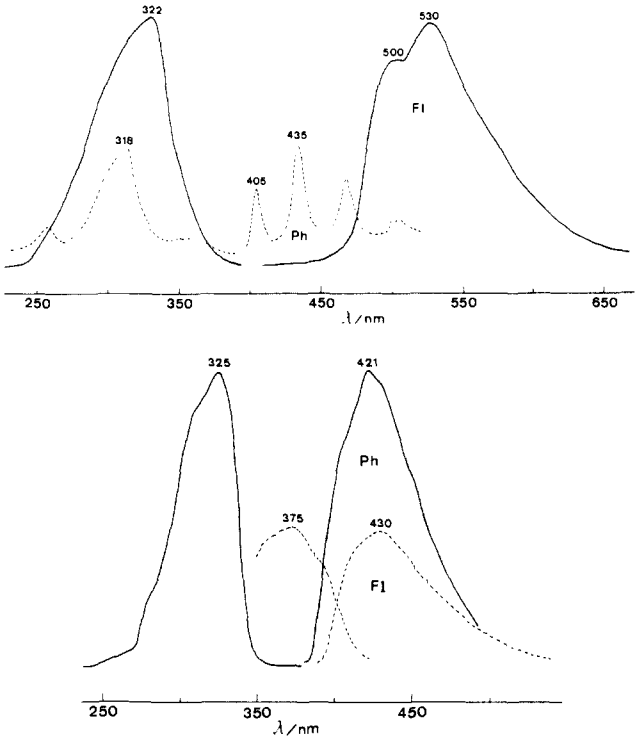

Figure 1. Emission and excitation spectra of 7HIN in (top (a)) MCH and (bottom (b)) EtOH + Tol observed at 77 K. All emission and excitation spectra were obtained by excitation and observation at the peak bands, respectively. Two kinds of emissions, Fl (fluorescence) and Ph (phosphorescence), were obtained in both solvents.

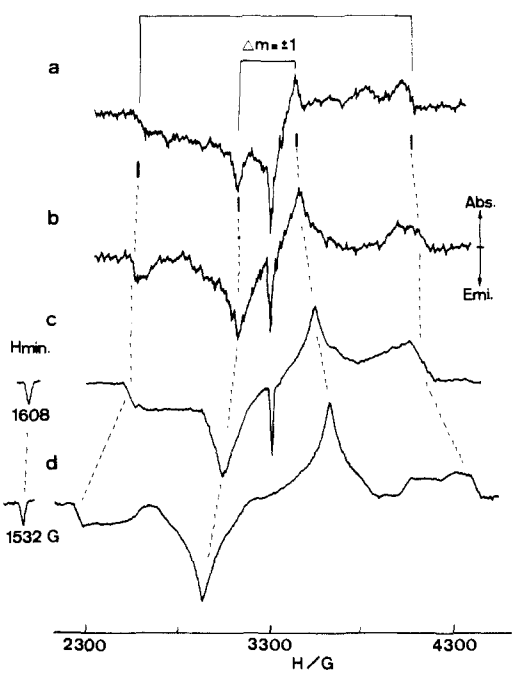

Figure 2. Time-resolved EPR spectra in MCH at 77 K and 0.4 μs after the laser pulse for (a) OHBA, (b) OHAP, (c) 7HIN, and (d) SAM.

were observed as indicated in the figure. Polarities of the signals at these fields were E;E,E,A and A (E,EE/AA pattern) from low to high fields. Here E and A denote an emission and an absorption of a microwave, respectively. In order to find another pair of $\Delta m = \pm 1$ transitions and to determine the triplet sublevel schemes in the MCH rigid glass, we performed magnetophotoselection (MPS) experiments. Typical MPS spectra with $\vec{H} \| \vec{E}$ and $\vec{H} \perp \vec{E}$ are shown for 7HIN in Figure 3, where $\vec{H}$ and $\vec{E}$ denote the directions of the applied magnetic field and the transition dipole moment of 7HIN at 308 nm, respectively. In these spectra the third pair of the $\Delta m = \pm 1$ transitions (X_1) was clearly seen with

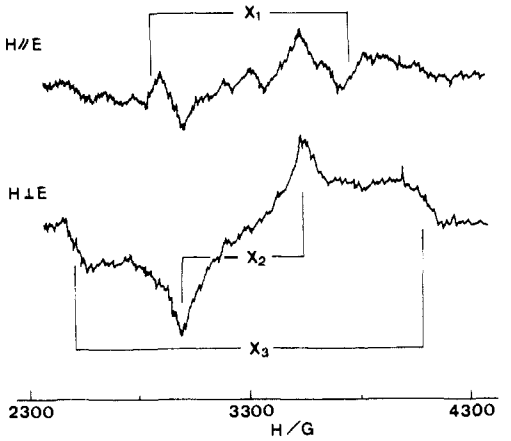

Figure 3. Magnetophotoselection spectra for 7HIN in MCH. The zero-field energies, X_1, X_2, and X_3, were obtained from the resonance fields of each canonical orientation.

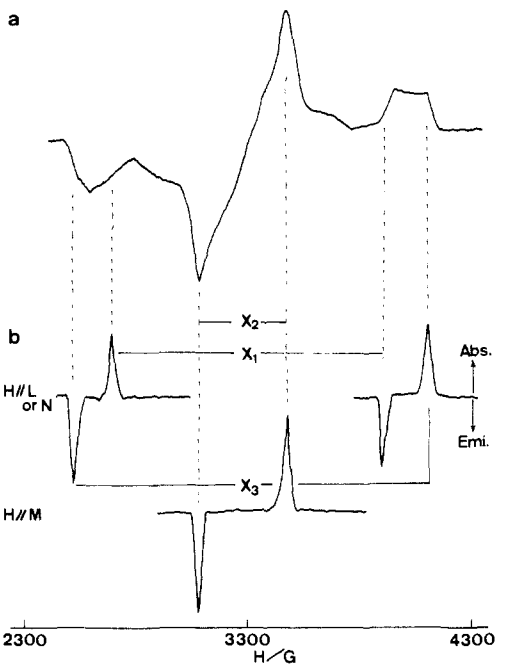

Figure 4. Time-resolved EPR spectra of OHAP in (a) powders and (b) a single crystal of durene at 77 K.

$\vec{H} \| \vec{E}$, and the relative intensities of the signals of the outermost pair (X_3) increased with $\vec{H} \perp \vec{E}$. Accordingly, we can conclude that the spectra show E,EAE/AEA patterns for these molecules in MCH.

In order to confirm the above results for the positions and polarities of the signals at the canonical orientations and to determine the directions of the principal axes of the zero-field (zf) tensors, we performed TREPR experiments for OHAP and 7HIN in single crystals of durene. We first observed the spectra in powders of mixed crystals, which closely resemble those in MCH, as typically shown for OHAP in Figure 4A. We then examined the angular dependence of the signals of OHAP and 7HIN by rotating the single crystal of durene so that $\vec{H}$ rotated within the *LM* (molecular) and *NM* planes of durene. Here the *L*, *M*, and *N* axes represent the long and short in-plane axes and the out-of-plane axis, respectively, as shown in Figure 5. In the durene crystal there are two molecules per unit cell whose *M* axes are nearly parallel to each other and *L* and *N* axes are mutually perpendicular.[11] Thus it is possible to rotate $\vec{H}$ approximately in the *LM* and *NM* planes simultaneously. The angular dependences of the signals for OHAP and 7HIN are shown in Figures

(11) Robertson, J. M. *Proc. R. Soc. London, Ser. A* **1933**, *141*, 594.

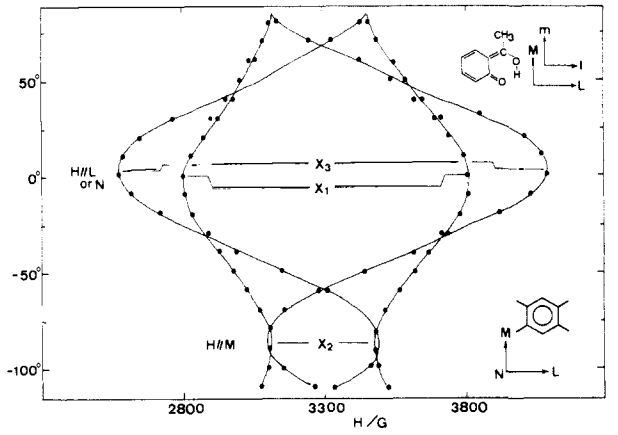

Figure 5. Angular dependence of the EPR signals for OHAP in a single crystal of durene. The observed canonical orientations are indicated.

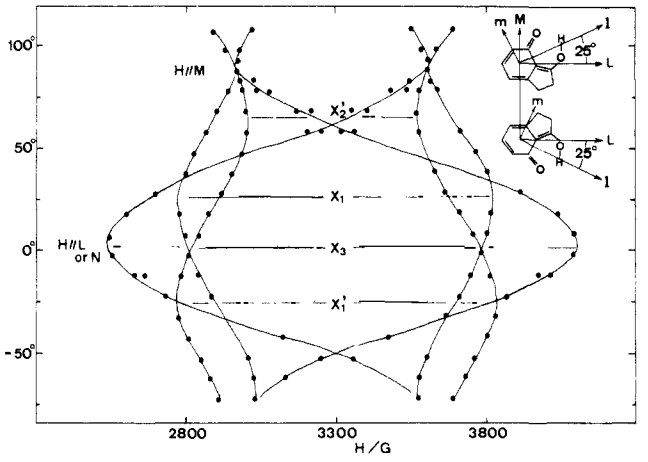

Figure 6. Angular dependence of the EPR signals for 7HIN in a single crystal of durene.

5 and 6, respectively. The signals at canonical orientations are shown for OHAP in Figure 4b. The resonance fields at the canonical orientations obtained in powders and in crystals were mutually consistent, showing that we were detecting correct canonical orientations in the single-crystal experiments. In the case of OHAP X_3 (outermost) and X_1 (intermediate), stationary points were obtained when $\vec{H}$ was approximately along the N or L axes of durene, whereas X_2 (innermost) stationary points were obtained with $\vec{H} \| M$. The polarities of the signals at the canonical orientations were EAE/AEA, in agreement with that in MCH. Despite the poor molecular symmetry, only the signals due to one pair of OHAP molecules were observed at every crystal orientation. In 7HIN the X_3 stationary points were obtained with $\vec{H} \| N$ or L, but now pairs of X_1 and X_2 stationary points were mutually separated by 50°. The polarities of the signals also showed an EAE/AEA pattern. Absolute values of zfs (X_1, X_2, and X_3) obtained from the resonance fields at the canonical orientations are summarized in Table II.

In EtOH + Tol the shapes of the TREPR spectra of OHAP and SAM are very similar to those in MCH, though the resonance fields for SAM at the canonical orientations are somewhat different from those in MCH. This indicates that in OHAP and SAM the major triplet species existing in the polar solvent are similar to those in MCH. In contrast, both the resonance fields and the polarities of the signals at the canonical orientations were quite different for OHBA and 7HIN in EtOH + Tol as shown in Figure 7. The OHBA spectrum shows the dominant E and A polarizations on the low- and high-field sides, respectively. The 7HIN spectrum gives rise to an AEA/EAE pattern. These spectra spread over wider regions of the magnetic field, indicating larger zfs. The zfs of 7HIN is given in Table II, but the zfs could not be determined accurately for OHBA in EtOH + Tol, because of the broad nature of the spectrum. When NaOH (10^{-2} M) was

Table II. Observed Zero-Field Energies and Zero-Field Splitting Parameters (GHz)

	OHBA	OHAP	7HIN	SAM
		MCH		
X_1	±1.11	±1.17	±1.02	±1.37
X_2	±0.28	±0.29	±0.46	±0.65
X_3	∓1.39	∓1.46	∓1.48	∓2.02
D^a	2.09	2.19	2.22	3.03
E	0.42	0.44	0.28	0.36
		EtOH + Tol		
X_1		±1.22	±2.13	±1.20
X_2		±0.31	±0.11	±0.33
X_3		∓1.53	∓2.24	∓1.53
D		2.30	3.36	2.30
E		0.46	1.01	0.44
		Durene		
X_1		±1.12	±0.92	
X_2		±0.35	±0.56	
X_3		∓1.46	∓1.48	
D		2.20	2.22	
E		0.39	0.18	

[a] See text for the definition of D and E.

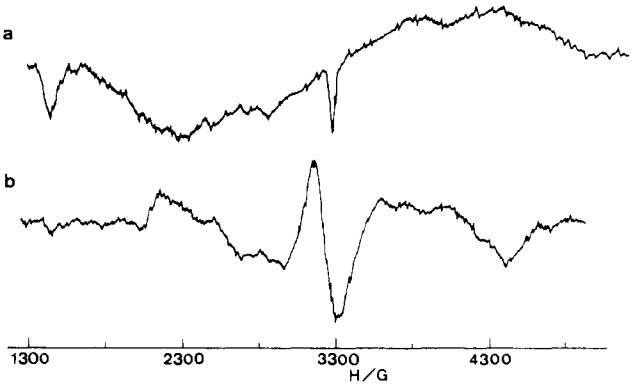

Figure 7. Time-resolved EPR spectra of (a) OHBA and (b) 7HIN in a mixed solvent of EtOH and Tol (1:1) at 77 K.

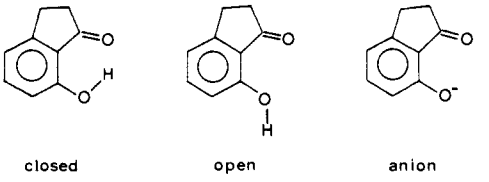

Figure 8. Possible conformers of the keto form and anion for 7HIN.

added to the 7HIN/(EtOH + Tol) system, the TREPR spectrum having an AEA/EAE pattern changed to a spectrum which is very similar to that observed in MCH (E,EAE/AEA pattern).

Discussion

1. Emission Properties and TREPR Spectra. In previous work we suggested that intramolecularly hydrogen-bonded closed conformers (Figure 8) emit enol fluorescence, whereas open conformers (Figure 8) emit phosphorescence.[5] The emission properties summarized in Table I show that the main species existing in MCH are closed conformers, with coexisting open conformers in OHBA and 7HIN. In EtOH + Tol intermolecularly hydrogen-bonded open conformers emit keto type $^3\pi\pi^*$ phosphorescence in all cases, but closed conformers coexist in the cases of OHAP and SAM.

In the TREPR experiments we have observed the spectra having the same polarization pattern (E,EAE/AEA) for all the molecules studied in MCH, and OHAP and SAM in EtOH + Tol, though the resonance fields are somewhat different depending on the system. This polarization pattern is very different from those (E,EEE/AAA or E,EEA/AAE) for usual $^3\pi\pi^*$ and $^3n\pi^*$ keto type aromatic carbonyls expected from the known triplet sublevel schemes and populating rates.[12] It is important to note that the

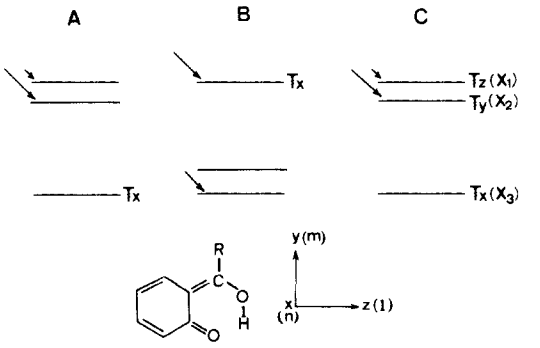

Figure 9. Possible zero-field schemes (A and B) and the fully determined scheme (C) for the triplet enols. (l, m, n) and (x, y, z) denote the molecular axes and the fine structure axes, respectively.

enol type fluorescence was always observed in these systems having the E,EAE/AEA type spectra. Therefore, we can safely conclude that we were observing the TREPR spectra of the excited triplet states of the enol type. In contrast, the polarization pattern of the TREPR spectra are different for OHBA (E,EEA/EAA) and 7HIN (AEA/EAE) in EtOH + Tol, in which the enol type fluorescence was not observed, and the $^3\pi\pi^*$ type phosphorescence and anion fluorescence were observed instead. When NaOH was added to the 7HIN/(EtOH + Tol) system, the anion emission increased and at the same time the TREPR spectrum changed drastically. These observations indicate that the TREPR spectra observed for OHBA and 7HIN in EtOH + Tol are likely due to keto type $^3\pi\pi^*$ triplet states.

Though the $^3n\pi^*$ type phosphorescence was observed in OHBA and 7HIN in MCH, no TREPR spectra of these species were detected, presumably because the zfs of these carbonyls are very large.[13] Also the TREPR spectra of the keto type $^3\pi\pi^*$ states of OHAP and SAM were not observed clearly in EtOH + Tol. The EPR spectra of these species may be broad and hidden under the strong signals of the enol triplet states.

2. Sublevel Schemes and Polarization Pattern. Enol Type Triplet States. We first discuss the sublevel schemes of the enol type triplet states. From the analysis of the TREPR spectra we obtained the polarization pattern of E,EAE/AEA and the absolute values of the zfs (Table II). On the basis of these results two possible zero-field sublevel schemes, A and B in Figure 9, are considered. The length of the arrows indicates the relative magnitude of the $S_1 \rightarrow T_i$ ($i = x, y, z$) intersystem crossing (isc) rate. The out-of-plane sublevel, T_x, is assigned as the farmost sublevel, either the bottom sublevel in A or the top one in B, by the MPS experiments as the following. The S_1 ($\pi\pi^*$) state is excited by the excimer laser (λ = 308 nm) and, therefore, $\vec{E}$ should be in the molecular (zy) plane. The result that the outermost pair of the $\Delta m = \pm 1$ transitions increased the intensities of the EPR signals with $\vec{H} \perp \vec{E}$ indicates that the outermost peaks correspond to those at $\vec{H} \| x$. Thus T_x is assigned as the farmost sublevel in Figure 9. This assignment was of course consistent with the result of the single-crystal experiments in which the outermost pairs of the $\Delta m = \pm 1$ transitions were obtained with $\vec{H} \| N$ or L of durene. Since the guest molecules are expected to replace the host molecules with their molecular planes parallel to each other, this indicates that the farmost sublevel is T_x or T_z.

In all planar $^3\pi\pi^*$ and $^3n\pi^*$ aromatic carbonyls T_x is known to be the bottom sublevel as in A.[12,13] The B type sublevel scheme was found in $^3n\pi^*$ aliphatic carbonyls, where the molecules are severely distorted from planarity.[14] Since the present molecules are nearly planar and $S_1 \rightarrow T_1$ isc predominantly populates in-plane sublevels, the enol type triplet states are considered to have the A type sublevel scheme. When we take account of the fact that the lowest singlet states of the enols are $\pi\pi^*$ in character and the magnitudes of the S–T splittings for $^3n\pi^*$ carbonyls ($\sim$2000 cm^{-1}) are much smaller than those ($\sim$8000 cm^{-1}) for $\pi\pi^*$ states, we can conclude that the T_1 states are $^3\pi\pi^*$ in character with the A type sublevel scheme.

We next try to assign the in-plane sublevels on the basis of the results of the single-crystal experiments. Though the molecular symmetry of OHAP is poor, OHAP is considered to go into the durene crystal with its long (l) axis nearly parallel to the L axis of durene. In fact, it is known that molecules with similar structures such as 1-methyl- and 1-bromonaphthalenes replace durene in this fashion[15,16] (θ = 8° and 0°, respectively; θ is the angle between L and l). The results of the angular dependence studies shown in Figures 5 and 6 and the assignment of the X_3 stationary points being observed with $\vec{H} \| N(x)$ show that X_1 and X_2 were obtained with $\vec{H}$ approximately parallel to the L and M axes of durene, respectively. Combining these results, we consider that the directions of the in-plane (z and y) principal axes of the zf tensor nearly coincide with the long (l) and short (m) axes of OHAP, respectively, with the T_z sublevel being the top one. Thus the zf scheme of the enol triplet is now determined as shown in Figure 9C. This assignment seems to be consistent with the result for 7HIN. 7HIN with a bulkier group attached to the carbonyl group may go into durene with the l axis deviating from the L axis (l and m axes are taken as in the case of OHAP shown in Figure 5). If the l direction deviates from the L direction by ±25° as shown in Figure 6, we expect to observe two pairs of signals mutually separated by 50° by rotating $\vec{H}$ in the molecular plane of one type of durene. This is exactly what was observed as shown in Figure 6. Here the out-of-plane x axis was found to be parallel to the N axis of durene, confirming that only the in-plane axes are rotated in the molecular plane (θ = 25°).

The zfs (D and E) determined from the spin Hamiltonian

$$\mathcal{H} = g\beta\vec{H}\cdot S + D(S_x^2 - \tfrac{1}{3}\vec{S}^2) + E(S_z^2 + S_y^2)$$

are given in Table II. A notable feature about the zfs of the enol triplet states is that they are rather small, considerably smaller than those of the molecules of comparable sizes such as substituted benzaldehydes,[12,13] substituted benzenes,[17] and naphthalenes.[18] Since the $^3n\pi^*$ states are located much higher in energy than the T_1 ($^3\pi\pi^*$) states, contribution to zfs by the second-order effect of the spin–orbit coupling is negligibly small. Therefore, the magnitudes of the zfs are determined by spin–spin interactions, and their contributions must be rather small in these systems.

The above sublevel assignment leads to an interesting observation about the dominant populating rates. The rate of proton transfer is considered to be faster than the intersystem crossing rate in the keto form, and the enol triplet state is expected to be formed from the enol singlet state. This expectation is supported by the result of the present work as discussed in the last section. The polarization pattern observed in the TREPR spectra of all the enol type triplet states indicates that the T_y (middle) sublevels are predominantly populated. This is quite different from the cases of keto type $^3\pi\pi^*$ and $^3n\pi^*$ carbonyls so far studied in which the top (T_z; z axis is along the C=O direction) sublevels are dominantly populated by a mechanism involving spin–orbit coupling between the $^3\pi\pi^*$ and $^1n\pi^*$ states.[12] Thus the observed polarization characteristics also exclude the possibility of the T_1 state of the enol being a $^3n\pi^*$ state.

In the present systems the z direction is considered to be about 30° away from the C=O direction. If the same spin–orbit mechanism is operative in the present systems, the T_z sublevels should be populated more than the T_y sublevels. The observed polarization indicates that this is not the case. This observation may be rationalized in the following. In the keto type $^3\pi\pi^*$ aromatic carbonyls, $^1n\pi^*$ states are the S_1 states or are located

(12) Cheng, T. H.; Hirota, N. *Mol. Phys.* **1974**, *27*, 281.
(13) Nishimura, A. M.; Tinti, D. S. *Chem. Phys. Lett.* **1972**, *13*, 278.
(14) (a) Shain, A. L.; Sharnoff, M. *Chem. Phys. Lett.* **1972**, *16*, 503. (b) Baba, M.; Hirota, N. *Chem. Phys. Lett.* **1979**, *64*, 321. (c) Gehrtz, M.; Brauchle, C.; Voitlander, J. *Mol. Phys.* **1984**, *53*, 769.
(15) Rodgers, E. G.; Vincent, J. S. *J. Chem. Phys.* **1970**, *52*, 4627.
(16) Kothandaraman, G.; Pratt, D. W. *J. Chem. Phys.* **1975**, *63*, 3337.
(17) Vergragt, Ph. J.; Kooter, J. A.; van der Waals, J. H. *Mol. Phys.* **1979**, *53*, 769.
(18) Nishi, N.; Matsui, K.; Kinoshita, M.; Higuchi, J. *Mol. Phys.* **1979**, *38*, 1.

close to the S_1 states. In these systems the mechanism involving the spin–orbit coupling with $^1n\pi^*$ or $^3n\pi^*$ states is effective. On the other hand, in the enol tautomers the $^1n\pi^*$ and $^3n\pi^*$ states are probably much higher in energy than the S_1 ($\pi\pi^*$) states, making this mechanism less effective. In such systems the mechanism involving the spin–orbit coupling with $^1\sigma\pi^*$ ($^1\pi\sigma^*$) states may become more effective, making the populating rate into T_y the largest. In this connection it is notable that the relative importance of the mechanisms involving $^1\sigma\pi^*$ ($^1\pi\sigma^*$) states in the $T_1 \rightarrow S_0$ decay processes in the $^3\pi\pi^*$ aromatic carbonyls increases as the $^3n\pi^*$–$^3\pi\pi^*$ energy separation increases.[19]

OHBA and 7HIN in Polar Solvents. The emission spectra obtained in these systems indicate that the main triplet species present are $^3\pi\pi^*$ in character. Although accurate values of zfs could not be determined in the case of OHBA in EtOH + Tol, the spectrum (Figure 7a) is consistent with that expected from the zfs and the sublevel populating rate of a $^3\pi\pi^*$ carbonyl such as benzaldehyde ($D = -(3/2)X = 4.14$ GHz, $E = 0.26$ GHz, and T_z being most populated) in benzoic acid.[20] The zf parameters of 7HIN are similar to those of 1-indanone ($D = 3.24$ GHz, $E = 1.29$ GHz) in dimethoxybenzene,[21] and are reasonable as those of a keto type $^3\pi\pi^*$ aromatic carbonyl. However, the polarization is unusual, because the observed spectral pattern requires that the T_x sublevel is dominantly populated. If the molecule is severely distorted from planarity, dominant population into T_x becomes possible, but this possibility seems unlikely in the present case. Another possibility is that this is due to an artifact caused by our experimental procedure. Since the triplet lifetime is remarkably longer than the repetition period (80 ms) of the laser excitation, the observed pattern may not represent the correct populating rate due to the $S_1 \rightarrow T_1$ ISC.

3. Triplet Species Involved and Enolization Process. It is notable that the main emitting species differ considerably depending on the molecule despite the similarities of the structures. In MCH intramolecularly hydrogen-bonded closed conformers of the keto type are the main species, but, as discussed in the previous paper, this species is converted to the open conformer by UV irradiation in OHBA. This conversion does not take place appreciably in other systems. 7HIN in MCH emits $^3n\pi^*$ type phosphorescence due to the open conformer. Presumably weaker hydrogen bonding due to a longer O–H···O distance allows the presence of the open conformer even in MCH. Though intermolecularly hydrogen-bonded open conformers are the main species for all the molecules in EtOH + Tol, closed conformers exist in OHAP and SAM. In 7HIN a weaker intramolecular hydrogen bonding makes the intramolecularly hydrogen-bonded close conformers less favorable. In OHAP and SAM steric hindrance may make the open conformers less stable, allowing coexistence of the closed conformers even in EtOH + Tol.

Finally, we discuss whether enolization takes place in the singlet state or the triplet state. First we note that the TREPR spectrum of the T_1 state of the 7HIN anion is very similar to that of the enol triplet state of 7HIN, including its zfs and polarization characteristics. Then the electronic structures of the anion and the enol must be similar. Since only one species is involved in the excitation and decay process of the anion (Figure 8), T_1 of the anion is formed from S_1 of the anion via isc. The fact that the polarization characteristics of the enol and anion triplets are similar strongly indicates that T_1 of the enol is also formed from S_1 of the enol via isc and enolization takes place in the singlet state. If enolization occurs in the triplet state, the polarization pattern of the enol should be different from that of the anion. The $S_1 \rightarrow T_1$ isc in the keto type carbonyl populates the T_z sublevel predominantly, and this polarization should be preserved in the process of enolization. This should result in a larger population of T_z than T_y, contrary to observation.

Conclusion and an Additional Remark

We have observed transient EPR spectra of the T_1 states of intramolecularly hydrogen-bonded OHBA, OHAP, SAM, and 7HIN in MCH and EtOH + Tol as well as in mixed crystals of durene. The EPR spectra observed in MCH and durene are identified as those of the triplet states of the enol tautomers which are nonphosphorescent and short-lived. The spectra are characterized by small zfs and unique polarization patterns. The sublevel schemes and the directions of the principal axes of the zf tensors were determined. A possible explanation for the unusual polarization is suggested. In EtOH + Tol spectra of the enol triplet states were also observed for OHAP and SAM, but spectra of the keto type carbonyls were obtained for OHBA and 7HIN. The main species present under various conditions are discussed on the basis of the EPR and emission spectra. It was concluded that the enolization takes place in the singlet state.

After this work was completed, a short paper on the triplet enols generated from *o*-methylacetophenone (OMA) and related compounds appeared.[22] Small values of the zfs are very similar to our values, but the polarization pattern found for OMA is very different from those found here, presumably suggesting that different mechanisms are involved in the formation of the triplet enols.

Acknowledgment. We thank Professor H. Iwamura of the Institute of Molecular Science (now at the University of Tokyo) for a gift of 7HIN.

Registry No. OHBA, 90-02-8; OHAP, 118-93-4; SAM, 65-45-2; MS, 119-36-8; 7HIN, 6968-35-0.

(19) (a) Harrigan, E. T.; Chakrabarti, A.; Hirota, N. *J. Am. Chem. Soc.* **1976**, *98*, 3460. (b) Yamada, Y.; Yamauchi, S.; Hirota, N. *Bull. Chem. Soc. Jpn.* **1982**, *55*, 2046.
(20) Nagaoka, S.; Hirota, N. *J. Chem. Phys.* **1981**, *74*, 1637.
(21) Niizuma, S.; Hirota, N. *J. Phys. Chem.* **1978**, *82*, 453.
(22) Akiyama, K.; Ikegami, Y.; Tero-Kubota, S. *J. Am. Chem. Soc.* **1987**, *109*, 2538.